APPLIED PHYSICS

# Coherent Förster resonance energy transfer: A new paradigm for electrically driven quantum dot random lasers

Tien-Lin Shen[1]*, Han-Wen Hu[2]*, Wei-Ju Lin[2]*, Yu-Ming Liao[2], Tzu-Pei Chen[2], Yu-Kuang Liao[3], Tai-Yuan Lin[4], Yang-Fang Chen[2†]



**The many distinct advantages of random lasers focused efforts on developing a breakthrough from optical pumping to electrical pumping. However, progress in these is limited due to high optical loss and low gain. In this work, we demonstrate an electrically pumped quantum dot (QD) random laser with visible emission based on a previously unexplored paradigm named coherent Förster resonance energy transfer (CFRET). In the CFRET process, when a coherent photonic mode is formed because of multiple scattering of the emitted light traveling in mixed donor and acceptor QDs, the donor QDs not only serve as scattering centers but are also enable coherent energy transfer to acceptor QDs. Therefore, the laser action can be easily achieved, and the lasing threshold is greatly reduced. Our approach of electrically pumped QD-based random lasers represents a substantial step toward a full-spectrum random laser for practical applications.**

## INTRODUCTION

Random lasing is a laser emission process that scatters light in a disordered system and leads to interference, optical gain, and lasing (*1*–*4*). The disordered system can be constructed by optical material with multiple scattering centers, which is easier to be fabricated compared with traditional lasers that normally need a strictly designed cavity and complicate the fabrication process (*5*–*7*). To leverage these advantages of a laser system not only notably decreases the cost of a random laser but also suppresses the spatial coherence of a laser mode, which makes it suitable for many potential applications, such as visible speckle-free imaging and stochastic super-resolution spectroscopy (*8*–*10*). In addition, random lasers based on scattering have a unique feature of broad angular distribution, which is highly preferable for lighting, imaging, display technologies (*11*), biomedical diagnosis (*12*, *13*), and visible light communication (*14*).

Electrical pumping is greatly desirable for practical applications of any laser systems. However, electrically driven random laser faces multiple challenges. To achieve optical gain through stimulated emission, optical scattering element, such as particles or grain boundaries, has to exist in active layers of a random laser, for example, grains in disordered polycrystalline thin films (*15*–*18*). This relatively poor structural quality would deteriorate electrical characteristics of a laser device. Therefore, most of the random laser studies to date are using optical pumping (*19*–*22*). In addition, a stable, low–defect density n-doping or p-doping material thin film for highly efficient homojunction random laser is difficult to prepare. To our knowledge, most electrically driven random lasers are still focusing on ZnO-based thin film heterostructures, which have a wide bandgap and large exciton-binding energy that lead to high-efficiency and low-threshold laser diodes (*23*, *24*). A breakthrough on electrically driven random laser with mid-infrared emission has also been demonstrated using quantum cascade laser heterostructures (*25*). Nonetheless, a study on random laser with visible light emission has not yet been reported. Moreover, quantum dots (QDs) have great potential for the development of light emitters because of their highly efficient quantum yield, tunable wavelength, and cost-effectiveness. It is well known that multiple-exciton gain is required to achieve population inversion in a QD. Under this condition, the nonradiative Auger process is enhanced, which limits the optical gain and increases the lasing threshold. Therefore, even though colloidal QDs have highly efficient photoluminescence (PL) because of quantum confinement effect and the search for electrically pumped random laser action based on QDs has attracted great attention, all the attempts failed to demonstrate this exciting expectation (*26*).

In this study, we have successfully demonstrated the first electrically driven QD random laser with visible emission at 630 nm based on a new paradigm named coherent Förster resonance energy transfer (CFRET). Colloidal nanocrystalline QDs have been regarded as nano-emitters for next-generation laser devices (*27*–*29*). The use of QDs provides flexibility of laser wavelength selection by merely changing the size of QDs, and other advantages including strong optical gain, low lasing threshold, and fabrication-wise features with low-cost synthesis, and scalability in mass production because of solution-based characteristics (*30*–*32*). Förster resonance energy transfer (FRET), which involves nonradiative energetic coupling from energy donor to neighboring energy acceptor via dipole-dipole interaction, has been well characterized in published research and shows its potential value to many applications including biosensing, solar energy harvesting, and biomolecular conformation studies (*33*–*37*). The underlying mechanism of CFRET is to couple FRET process with a coherent photonic mode formed by multiple scattering, which enables optical gain to be elevated and enhances scattering simultaneously, providing strong coherent feedback for laser action to occur. To illustrate the working mechanism of our proposed CFRET process, following the principle of FRET, QDs with two different sizes having appropriate absorption and emission spectra were chosen as energy donors and acceptors,

[1]Graduate Institute of Applied Physics, National Taiwan University, Taipei 10617, Taiwan. [2]Department of Physics, National Taiwan University, Taipei 10617, Taiwan. [3]Department of Electro-physics, National Chiao Tung University, Hsinchu 30010, Taiwan. [4]Institute of Optoelectronic Sciences, National Taiwan Ocean University, Keelung 202, Taiwan.
*These authors contributed equally to this work.
†Corresponding author. Email: yfchen@phys.ntu.edu.tw

by which higher optical gain can be achieved (*38*, *39*). In addition, self-assembled QD clusters can serve as scattering centers to induce multiple scattering for the formation of coherent loops. Therefore, the donor QDs play two important roles simultaneously, including to serve as scattering centers and to transfer energy coherently. Moreover, to achieve electrically pumped QD laser, suitable design of electron and hole transport layers (HTLs) are required. Through the combination of all the important factors described above, a QD-based random laser with high emission intensity, angular independence, and high stability has been successfully demonstrated. The new paradigm shown here can be applied to many other QD systems to generate high-performance optoelectronic devices. The results presented here have not yet been realized in previous studies, which could have great impact in both academia and industry.

## RESULTS

### Structure and electrical performance of QD random laser

Figure 1A shows a schematic illustration of the QD-based random laser. The device is fabricated on indium tin oxide (ITO) glass substrate and solution-processed HTLs, consisting of poly(ethylenedioxythiophene): polystyrene sulphonate (PEDOT:PSS), poly[*N*,*N*9-*bis*(4-butylphenyl)-*N*,*N*9-*bis*(phenyl)-benzidine] (poly-TPD), poly(9-vinlycarbazole) (PVK), a 50-nm-thick layer of CdSe QD mixture with two different sizes, and a layer of ZnO nanoparticles with 160-nm thickness as electron transport layer. A scanning electron microscopy (SEM) cross-sectional image of the random laser is shown in Fig. 1B, evidently exhibiting QD and ZnO nanoparticle layers. Figure 1C shows a top-view SEM image over the active layer of the random laser assembled by CdSe QDs. Individual QDs can been seen in the SEM image. The inset of Fig. 1C is the photo of the random laser during device operation under electrical pumping, which shows a high emission intensity of red light.

The optimized performance of QD-based random laser was achieved by the device with a QD mixture consisting of QDs with 540-nm emission wavelength as the energy donor and those with 630-nm emission wavelength as the energy acceptor, and both of them were homogeneously mixed with equal amount. The ZnO nanoparticle layer is used as the electron transport layer because of its high mobility, suitable energy band, and simple solution processibility, while PEDOT:PSS/poly-TPD/PVK trilayers were used as HTLs to facilitate hole transport into the active layer and achieve charge balance under current injection. Figure 2A shows a schematic illustration of a flat-band energy level diagram of the device (*40*–*42*). Figure 2B shows current-voltage (*I*-*V*) curve of the random laser device, in which the turn-on voltage is found at 1.7 V with a low leakage current. This result confirms that heterojunction with the QDs' active layer has been fabricated successfully.

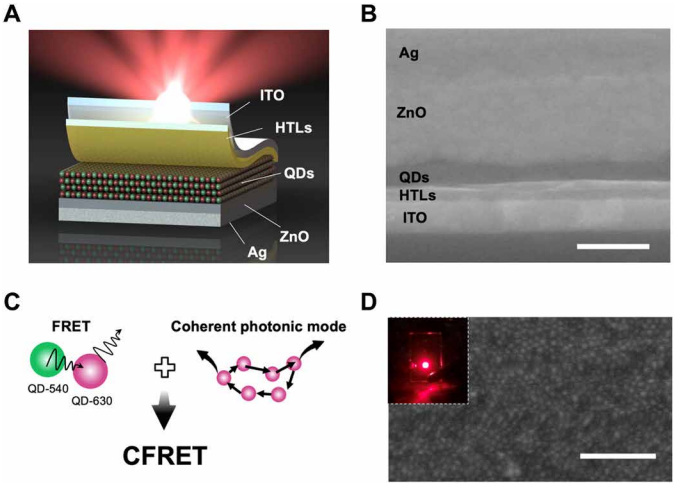


**Fig. 1. Structure of the QD random laser device.** (**A**) Schematic of the QD random laser device. (**B**) Side-view SEM image of the device structure showing each layer is well deposited. Scale bar, 200 nm. (**C**) Schematic illustration of CFRET. (**D**) SEM topography of the mixture QD film. Scale bar, 100 nm. The inset shows the real photo of the red-light emission from the QD random laser device.

### Electroluminescence measurements of laser characteristics

Figure 3A shows the electroluminescence (EL) spectrum of the QD-based random laser device under continuous current injection. An EL emission peak with full width at half maximum (FWHM) of 40 nm was observed under a low injection current of 20 mA. As the injection current was increased to 40 mA, several sharp peaks with narrow FWHMs appeared, as shown in the spectrum, and among which, the strongest peak has an emission wavelength of 630 nm and linewidth of 1.9 nm. Peak intensity of the strongest emission is plotted as a function of injection current as shown in Fig. 3B, from which, a 35-mA threshold injection current is obtained. In addition, the monitored operating time in the lasing regime lasts for 6 min. We believe that a longer lifetime can be expected because the laser action can be repeated several times. Both of the threshold behaviors of the detected emission intensity and FWHM provide a signature of laser action. In addition, the occurrence of multiple sharp peaks is very similar to the observed random laser action in a previous report (*6*, *43*, *44*).

### Evidence of random laser

Figure 4 displays laser emission spectra of the random laser device under 40-mA injection current collected at different angles, spanning from −45° to +45° with respect to surface normal. The angle-dependent EL spectra show that the sharp lasing peaks appear in all directions and exhibit the same feature with respect to the measured angle. Broad-angle emission is a distinct evidence of random lasers, which distinguishes themselves from conventional lasers that are highly directional. The angle-dependent measurement also excludes the possibility that the observed sharp peaks arise from the cavity resonance in between the top and bottom electrodes. In addition, as in the cross-sectional SEM image shown in Fig. 1B, the thickness of the device in-between the top and bottom electrodes is much less than the emission wavelength; hence, the possibility of a single resonator formed by multilayer stacking in the device can be eliminated. This result is also supported by the fact that as the QD-based device contains pure 630- or 540-nm QDs, no laser action and interference patterns are observed under high injection current, as respectively exhibited in figs. S1 and S2.

### PL measurements of QD mixture layer

To further investigate the lasing mechanism of the QD-based random laser, the PL spectra of the QD mixture active layer is analyzed. Random lasing can be observed under optical excitation, as shown in fig. S3A. Peak intensity of the emission is plotted as a function of pumping power density as shown in fig. S3B, from which evident sharp PL peaks can be observed under excitation intensity of 35.65 kW/cm$^2$, and multiple lasing modes become more pronounced as pumping

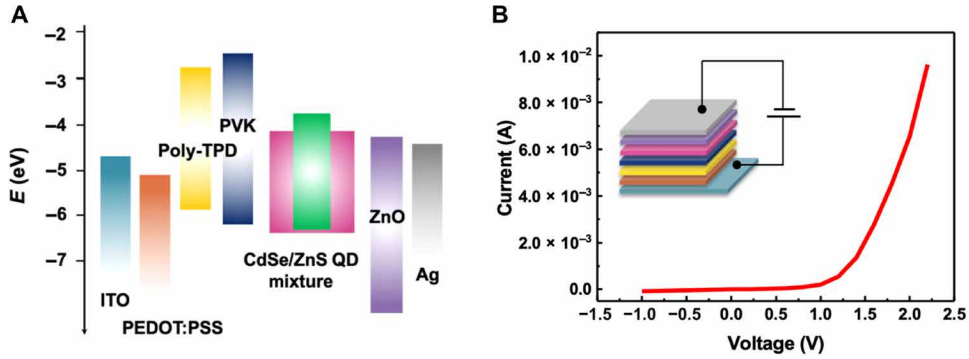


**Fig. 2. Energy band diagram and *I-V* characteristics of the QD random laser device.** (**A**) Flat-band energy level diagram. (**B**) *I-V* characteristic of the QD random laser device. Positive bias is applied on the ITO side.

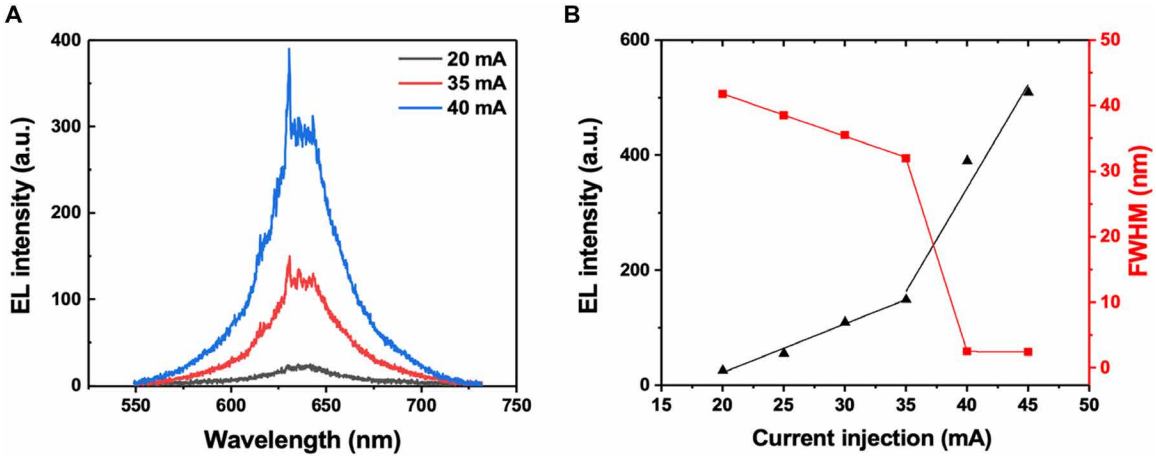


**Fig. 3. Random laser emission characteristics.** (**A**) Electroluminescence spectra of the laser device operated under different current injection. Lasing characteristics are observed at 40 mA. (**B**) Emission peak intensity and FWHM as a function of injection current. a.u., arbitrary unit.

power is increased. The laser action was not observed in the device containing only one kind of QDs, which again provides an additional evidence to confirm that the laser action does not arise from cavity resonance. The finding from the PL measurements is consistent with the results of the EL measurements. On the basis of both EL and PL measurements, the mechanism of laser action through internal cavity formed by multilayers in the device can be excluded. In addition, it reveals the fact that multiple scattering in the active layer is the most plausible mechanism for the observed laser action. Moreover, the surface morphology of the QD mixture active layer is investigated by atomic force microscopy (AFM) as shown in fig. S5. Multiple QD clusters are observed in the AFM image, which supports the fact that QD clusters can serve as scattering centers, leading to multiple scattering for the formation of coherent photonic mode and the subsequent random lasing.

Random lasing was absent in the device containing QDs with single emission wavelength and was only observed on the device consisting of QD mixture with 540- and 630-nm emission wavelength. This interesting result is very important and desires a clearer understanding, which can be well interpreted by the combination of several factors as described below. First, reabsorption of QD emission in the active layer can notably decrease optical gain, which is a crucial factor to suppress the occurrence of laser action. The reabsorption can be quenched in 540-nm QDs mixed with 630-nm QD layer. In the QD mixture active layer, photons with 630-nm lasing wavelength cannot be absorbed by 540-nm QDs, which guarantees that QDs with 540-nm emission can only serve as scattering centers without absorption. Therefore, the effective multiple scattering provided by 540-nm QDs is enabled to enhance optical gain in the active layer and lead to the observed random laser action. Furthermore, CFRET also plays a very important role in our observed laser action.

## DISCUSSION

### The mechanism of CFRET

In the conventional FRET process, efficient energy transfer from energy donor to energy acceptor requires deep spectral overlap of the donor and acceptor pair. Figure 5A shows the emission spectra of the energy donor and energy acceptor corresponding to 540-nm QDs (black line) and 630-nm QDs (red line) used in our study, along with the absorption spectrum of the 630-nm QD energy acceptor (blue line). Deep spectral overlap is shown in the spectra, indicating the possibility of intensive energy transfer from 540- to 630-nm QDs. Meanwhile, self-formed coherent photonic mode can occur for the emitted light traveling in the QD active layer because

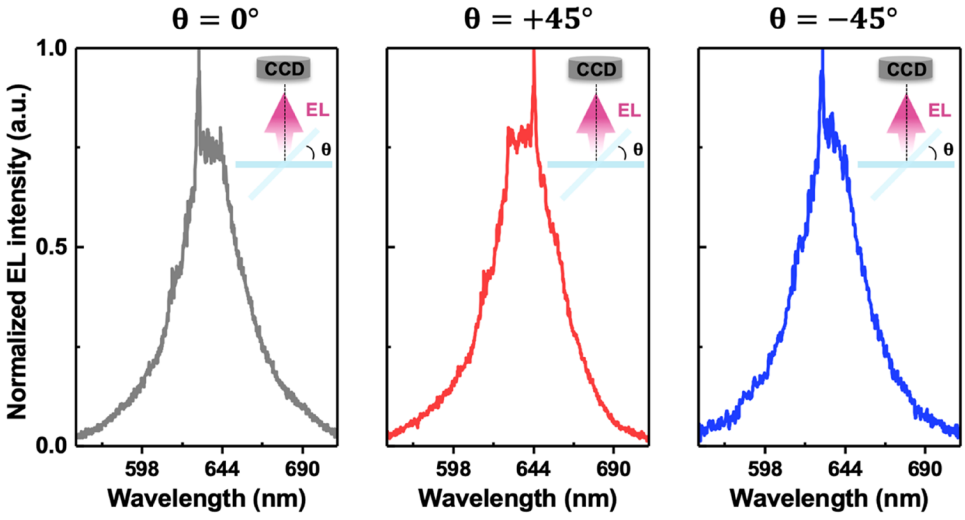


**Fig. 4. Angle-independent QD random laser characteristics.** The EL lasing spectra are observed at an angle of 0°, +45°, and −45° in the plane normal to the film. CCD (charge-coupled device) detect the laser signal and transfer into electrical signal.

of multiple scattering. In this particular instance, the donor QD scattering centers can transfer energy to acceptor QDs coherently, which will induce the so-called CFRET. CFRET will depopulate the excited state of the donor, resulting in a decreased probability of photon emission from donor and a shortened donor lifetime in the presence of an acceptor. It is expected that the energetic coupling from donor to acceptor causes increasing probability of fluorescence emission, leading to an extended acceptor lifetime. Time-resolved photoluminescence (TRPL) spectra were obtained and displayed in Fig. 5(B and C) to infirm the mechanism of CFRET. TRPL curves of 540- and 630-nm QDs are displayed in Fig. 5(B and C, respectively). TRPL curves of the QD mixture monitored at 540 and 630 nm have also been obtained, of which a decay curve of 540 nm is shown in Fig. 5B, while a decay curve of 630 nm is shown in Fig. 5C. According to the TRPL spectra, it shows that the lifetime of 540-nm QDs is decreased as they are mixed with 630-nm QDs and that of 630-nm QDs is increased as they are mixed with 530-nm QDs. These results are in agreement with the prediction based on the CFRET process. A number of optically pumped FRET-assisted random lasers have been studied recently (*45*–*51*). In all these studies, with the incorporation of donor molecules, the threshold of the random laser can be efficiently suppressed and the peak intensity can be enhanced compared with the nondoped one. The occurrence of random lasers is based on scattering media, such as polystyrene, polymer fibers, and latex particles, to achieve multiple scattering within the disordered structures. However, these scattering materials do not play any role in the FRET process. In stark contrast, in our study, the donor QDs not only assist the optical gain in the FRET process but also serve as the inherent scattering center for random lasers to occur. This unique feature enables us to find the coherent FRET phenomenon when the coherent photonic mode is formed because of multiple scattering, which was impossible to be observed in all previous reports. With a suitable design of donor QDs, such as band alignment and dots concentration, the lasing action can be easily achieved. This unique underlying mechanism therefore leads us to demonstrate the electrically pumped QD random laser.

To have a more quantitative analysis of the TRPL measurement, carrier lifetimes of each samples were acquired by biexponential fitting using Eq. 1 listed below. Fast component of double exponential TRPL decay of QDs is caused by the recombination of delocalized exciton in the internal core states (*52*, *53*), and slow component lifetime is attributed to the lifetime of carrier participating in the CFRET process. The lifetime of donor QDs is decreased from 20 to 12 ns, while that of acceptor QDs is increased from 22 to 40 ns, exhibiting large changes in the carrier lifetime of QDs in comparison with pristine QD samples and mixture QD samples, and showing CFRET from donor QDs to acceptor QDs. The carrier lifetime of donor QDs was used to calculate the CFRET efficiency through Eq. 2 as shown below, where $\tau_{DA}$ and $\tau_{D,}$ respectively, are the donor average fluorescence lifetimes in the presence and absence of acceptor, and $\eta_{FRET}$ is the CFRET efficiency. Forty percent of the CFRET efficiency is obtained by Eq. 2

$$I(t) = \alpha_1 e^{-\frac{t}{\tau_1}} + \alpha_2 e^{-\frac{t}{\tau_2}} \quad (1)$$

$$\eta_{CFRET} = 1 - \frac{\tau_{DA}}{\tau_D} \quad (2)$$

These changes in carrier lifetime indicate that CFRET occurs as an efficient energy transfer channel from 540- to 630-nm QDs. The carrier lifetime as a function of pumping power density is shown in Fig. 5D. As the pumping power density is increased, the lifetime of acceptor in the mixture QD thin film starts to decrease. This is because more existence of excitons is produced when increasing the pumping power density, which causes higher recombination rate; therefore, the carrier lifetime is reduced. When pumping power density is further increased beyond the threshold, additional photons are produced during scattering and causes drastic decrease in carrier lifetime. It provides an important clue that higher optical gain of QD mixture active layer leads to random lasing of QDs, compared with the active layer that solely contains 630-nm QDs, where random lasing is absent.

The occurrence of high optical gain at 630 nm in the device with the QD mixture active layer can also be understood by the band alignment. As shown in Fig. 2A, energy states of QDs are spatially sandwiched by PVK and ZnO with high bandgap energy, by which large potential barriers are built up at interfaces of QD layers against

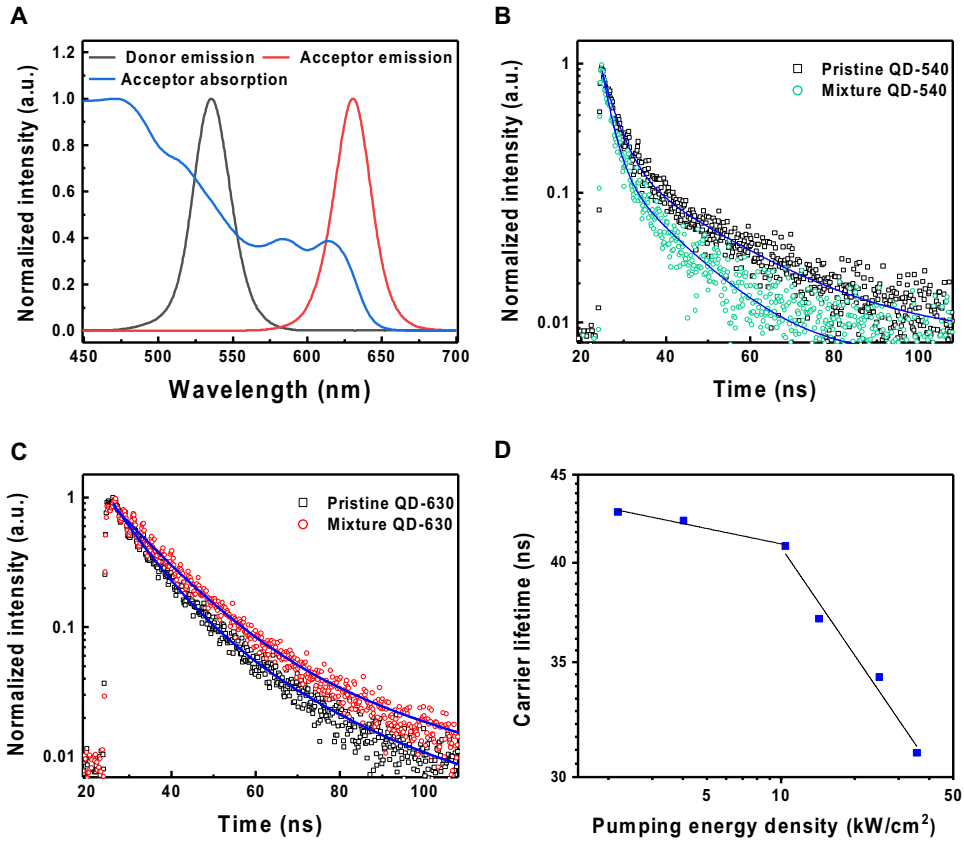


**Fig. 5. Characteristics of mixture QD thin film.** (**A**) Absorption and photoluminescence spectra of acceptor and emission spectrum of donor. (**B**) Time-resolved photoluminescence spectra of pristine and mixed QDs, monitored at 540 nm. **(C)** Time-resolved photoluminescence spectra of pristine and mixed QDs monitored at 630 nm. (**D**) Carrier lifetime as a function of pumping power density, monitored at 630 nm.

ZnO and PVK for the transport of holes and electrons, respectively. This helps confine carriers within QD active layers. Because the bandgap energy of 540-nm QDs is larger than that of 630-nm QDs, carriers can easily overflow from 540-nm QDs into 630-nm QDs and partially contribute to the enhanced emission from 630-nm QDs (*39*, *54*). Another energy transfer contribution is by radiative energy transfer from 540- to 630-nm QDs, which can also assist the optical gain of 630-nm QDs along with CFRET and carrier overflow. Last, it is worth noting that random lasers can occur in both closed photonic modes and open photonic modes induced by multiple scattering in a disordered medium. In open photonic modes, the emitted photons propagating in the gain medium only have intensity or energy feedback with a smooth spectral shape. In contrast, closed photonic modes are formed by coherent feedback when scattered light is trapped within closed loops in disordered nanostructures. For closed photonic modes, there exists a field or amplitude feedback, and the spectrum is superimposed by multiple sharp peaks. According to our measurements, the spectra do contain multiple sharp spikes with very narrow linewidth, which is more appropriate to be attributed to coherent closed photonic modes. Even though we only demonstrate the electrically pumped random laser action of QDs with closed photonic modes in our current study, our purposed mechanism shown here should also be applicable for the situation of open photonic modes based on the similar underlying energy transfer process.

In conclusion, we have demonstrated an electrically pumped QD random laser with visible light emission by implementing a new paradigm of CFRET. The active layer of visible light random laser is formed by QD mixture with energy donors and energy acceptors. Optical gain of all-QD active layer has been found to be enhanced by the combination of several factors, including suppression of reabsorption, CFRET process, deep spectral overlap of donor and acceptor pair, as well as suitable band alignment of each stacking layer. Particularly, in the CFRET process, when a coherent photonic mode is achieved through multiple scattering induced by donor QDs, energy transfer from donors to acceptors can occur coherently, which enables to efficiently enhance optical gain and generate laser action. This study demonstrates a "paradigm shift" of next-generation laser device for the development of electrically pumped QD-based random laser device, which should be very useful and timely toward potential applications spanning from display, to optical communication, to medical diagnosis.

## MATERIALS AND METHODS

### Device fabrication

ITO-coated glass substrates (sheet resistance, 15 ohm/sq) were first spin coated with PEDOT:PSS (Heraeus Clevios TM PH1000) solutions at 5000 rpm for 60 s and cured for 10 min in the ambient air. Then, poly-TPD (FMPV), dissolved in chlorobenzene (8 mg/ml) and PVK (Sigma-Aldrich; average Mn, 25,000 to 50,000), dissolved in toluene (1.5 mg/ml), were consecutively spin coated at 3000 rpm for 60 s and were baked at 120° and 150°C for 30 min after deposition

of each layer. The CdSe/ZnS core/shell QDs with octadecylamine ligand (Sigma-Aldrich 900220 and 900215) in toluene were mixed at the optimized ratio of 1/1 and were spin coated on the HTL at 500 rpm for 120 s to ensure forming uniform QD thin films during solvent evaporation. ZnO nanocrystals dispersed in isopropanol (15 mg/ml) were deposited at the speed of 1500 rpm for 60 s. Last, Ag electrodes (100 nm) were deposited by thermal evaporation system under $7 \times 10^{-7}$ to $8 \times 10^{-7}$ torr. It is worth noting that except for the evaporation of electrodes, devices were all solution processed in ambient air.

### Characterization

The EL lasing measurements were carried out by a high-resolution spectrometer Jobin Yvon iHR550 together with a continuous-current power source Keithley 2410 electrometer. For PL lasing measurements, spectra were recorded using a Horiba Jobin Yvon TRIAX 320 spectrometer, where a 374-nm pulsed laser was used as the pumping laser. The images for cross sections and morphology of the samples were taken by a JEOL JSM-6500F field emission scanning electron microscope under the acceleration voltage of 15 kV. AFM was used to analyze the morphology of the QD thin films. In addition, absorption spectra were measured by ultraviolet/visible/near-infrared spectrophotometer (PerkinElmer LAMBDA 750). The carrier lifetime was acquired by using a time-correlated single-photon counting spectrometer setup (FluoTime 300, PicoQuant GmbH).

## SUPPLEMENTARY MATERIALS

Supplementary material for this article is available at http://advances.sciencemag.org/cgi/content/full/6/41/eaba1705/DC1

## REFERENCES


1. D. Wiersma, Laser physics—The smallest random laser. *Nature* **406**, 132–133 (2000).
2. D. S. Wiersma, The physics and applications of random lasers. *Nat. Phys.* **4**, 359–367 (2008).
3. J. Bravo-Abad, M. Soljacic, Physics—A unified picture of laser physics. *Science* **320**, 623–624 (2008).
4. H. E. Tureci, L. Ge, S. Rotter, A. D. Stone, Strong interactions in multimode random lasers. *Science* **320**, 643–646 (2008).
5. S. W. Eaton, A. Fu, A. B. Wong, C. Z. Ning, P. D. Yang, Semiconductor nanowire lasers. *Nat. Rev. Mater.* **1**, 16028 (2016).
6. X. Y. Shi, Y. M. Liao, H. Y. Lin, P. W. Tsao, M. J. Wu, S. Y. Lin, H. H. Hu, Z. N. Wang, T. Y. Lin, Y. C. Lai, Y. F. Chen, Dissolvable and recyclable random lasers. *ACS Nano* **11**, 7600–7607 (2017).
7. A. Graf, M. Held, Y. Zakharko, L. Tropf, M. C. Gather, J. Zaumseil, Electrical pumping and tuning of exciton-polaritons in carbon nanotube microcavities. *Nat. Mater.* **16**, 911–917 (2017).
8. M. Barredo-Zuriarrain, I. Iparraguirre, J. Fernandez, J. Azkargorta, R. Balda, Speckle-free near-infrared imaging using a $Nd3^{+}$ random laser. *Laser Phys. Lett.* **14**, 106201 (2017).
9. B. Redding, M. A. Choma, H. Cao, Speckle-free laser imaging using random laser illumination. *Nat. Photonics* **6**, 355–359 (2012).
10. A. Boschetti, A. Taschin, P. Bartolini, A. K. Tiwari, L. Pattelli, R. Torre, D. S. Wiersma, Spectral super-resolution spectroscopy using a random laser. *Nat. Photonics* **14**, 177–182 (2019).
11. S. W. Chang, W. C. Liao, Y. M. Liao, H. I. Lin, H. Y. Lin, W. J. Lin, S. Y. Lin, P. Perumal, G. Haider, C. T. Tai, K. C. Shen, C. H. Chang, Y. F. Huang, T. Y. Lin, Y. F. Chen, A white random laser. *Sci. Rep.* **8**, 2720 (2018).
12. R. C. Polson, Z. V. Vardeny, Random lasing in human tissues. *Appl. Phys. Lett.* **85**, 1289–1291 (2004).
13. R. C. Polson, Z. V. Vardeny, Cancerous tissue mapping from random lasing emission spectra. *J. Opt.* **12**, 024010 (2010).
14. C. X. Wang, C. Zhu, C. Y. Lv, D. S. Li, X. Y. Ma, D. R. Yang, Electrically pumped random lasing from hydrothermal ZnO films of large grains. *Appl. Surf. Sci.* **332**, 620–624 (2015).
15. X. Y. Liu, C. X. Shan, S. P. Wang, Z. Z. Zhang, D. Z. Shen, Electrically pumped random lasers fabricated from ZnO nanowire arrays. *Nanoscale* **4**, 2843–2846 (2012).
16. F. Gao, M. M. Morshed, S. B. Bashar, Y. D. Zheng, Y. Shi, J. L. Liu, Electrically pumped random lasing based on an Au-ZnO nanowire Schottky junction. *Nanoscale* **7**, 9505–9509 (2015).
17. Y. J. Lu, C. X. Shan, M. M. Jiang, G. C. Hu, N. Zhang, S. P. Wang, B. H. Lia, D. Z. Shen, Random lasing realized in n-ZnO/p-MgZnO core-shell nanowire heterostructures. *CrystEngComm* **17**, 3917–3922 (2015).
18. S. Chu, M. Olmedo, Z. Yang, J. Y. Kong, J. L. Liu, Electrically pumped ultraviolet ZnO diode lasers on Si. *Appl. Phys. Lett.* **93**, 181106 (2008).
19. S. F. Yu, Electrically pumped random lasers. *J. Phys. D. Appl. Phys.* **48**, 483001 (2015).
20. S. Caixeiro, M. Gaio, B. Marelli, F. G. Omenetto, R. Sapienza, Silk-based biocompatible random lasing. *Adv. Opt. Mater.* **4**, 998–1003 (2016).
21. F. Luan, B. B. Gu, A. S. L. Gomes, K. T. Yong, S. C. Wen, P. N. Prasad, Lasing in nanocomposite random media. *Nano Today* **10**, 168–192 (2015).
22. Z. X. Wang, X. G. Meng, S. H. Choi, S. Knitter, Y. L. Kim, H. Cao, V. M. Shalaev, A. Boltasseva, Controlling random lasing with three-dimensional plasmonic nanorod metamaterials. *Nano Lett.* **16**, 2471–2477 (2016).
23. E. S. P. Leong, S. F. Yu, UV random lasing action in p-SiC(4H)/i-ZnO-SiO2 nanocomposite/n-ZnO : Al heterojunction diodes. *Adv. Mater.* **18**, 1685–1688 (2006).
24. H. Zhu, C. X. Shan, B. Yao, B. H. Li, J. Y. Zhang, Z. Z. Zhang, D. X. Zhao, D. Z. Shen, X. W. Fan, Y. M. Lu, Z. K. Tong, Ultralow-threshold laser realized in zinc oxide. *Adv. Mater.* **21**, 1613–1617 (2009).
25. H. K. Liang, B. Meng, G. Z. Liang, J. Tao, Y. D. Chong, Q. J. Wang, Y. Zhang, Electrically pumped mid-infrared random lasers. *Adv. Mater.* **25**, 6859–6863 (2013).
26. J. Yu, S. Shendre, W.-k. Koh, B. Liu, M. Li, S. Hou, C. Hettiarachchi, S. Delikanli, P. Hernández-Martínez, M. D. Birowosuto, H. Wang, T. Sum, H. V. Demir, C. Dang, Electrically control amplified spontaneous emission in colloidal quantum dots. *Sci. Adv.* **5**, eaav3140 (2019).
27. E. U. Rafailov, M. A. Cataluna, W. Sibbett, Mode-locked quantum-dot lasers. *Nat. Photonics* **1**, 395–401 (2007).
28. A. Nurmikko, What future for quantum dot-based light emitters? *Nat. Nanotechnol.* **10**, 1001–1004 (2015).
29. J. Tatebayashi, S. Kako, J. F. Ho, Y. Ota, S. Iwamoto, Y. Arakawa, Room-temperature lasing in a single nanowire with quantum dots. *Nat. Photonics* **9**, 501–505 (2015).
30. Y. Shirasaki, G. J. Supran, M. G. Bawendi, V. Bulovic, Emergence of colloidal quantum-dot light-emitting technologies. *Nat. Photonics* **7**, 13–23 (2013).
31. C. Dang, J. Lee, C. Breen, J. S. Steckel, S. Coe-Sullivan, A. Nurmikko, Red, green and blue lasing enabled by single-exciton gain in colloidal quantum dot films. *Nat. Nanotechnol.* **7**, 335–339 (2012).
32. J. Kwak, W. K. Bae, D. Lee, I. Park, J. Lim, M. Park, H. Cho, H. Woo, D. Y. Yoon, K. Char, S. Lee, C. Lee, Bright and efficient full-color colloidal quantum dot light-emitting diodes using an inverted device structure. *Nano Lett.* **12**, 2362–2366 (2012).
33. A. R. Clapp, I. L. Medintz, H. Mattoussi, Forster resonance energy transfer investigations using quantum-dot fluorophores. *ChemPhysChem* **7**, 47–57 (2006).
34. X. Qiu, N. Hildebrandt, Rapid and multiplexed microRNA diagnostic assay using quantum dot-based forster resonance energy transfer. *ACS Nano* **9**, 8449–8457 (2015).
35. S. Choi, H. Jin, J. Bang, S. Kim, Layer-by-layer quantum dot assemblies for the enhanced energy transfers and their applications toward efficient solar cells. *J. Phys. Chem. Lett.* **3**, 3442–3447 (2012).
36. L. Yuan, W. Y. Lin, K. B. Zheng, S. Zhu, FRET-based small-molecule fluorescent probes: Rational design and bioimaging applications. *Acc. Chem. Res.* **46**, 1462–1473 (2013).
37. L. Albizu, M. Cottet, M. Kralikova, S. Stoev, R. Seyer, I. Brabet, T. Roux, H. Bazin, E. Bourrier, L. Lamarque, C. Breton, M. L. Rives, A. Newman, J. Javitch, E. Trinquet, M. Manning, J. P. Pin, B. Mouillac, T. Durroux, Time-resolved FRET between GPCR ligands reveals oligomers in native tissues. *Nat. Chem. Biol.* **6**, 587–594 (2010).
38. H. Z. Siboni, B. Sadeghimakki, S. Sivoththaman, H. Aziz, Very high brightness quantum dot light-emitting devices via enhanced energy transfer from a phosphorescent sensitizer. *ACS Appl. Mater. Interfaces* **7**, 25828–25834 (2015).
39. Y. R. Park, H. Y. Jeong, Y. S. Seo, W. K. Choi, Y. J. Hong, Quantum-dot light-emitting diodes with nitrogen-doped carbon nanodot hole transport and electronic energy transfer layer. *Sci. Rep.* **7**, 46422 (2017).
40. B. S. Mashford, M. Stevenson, Z. Popovic, C. Hamilton, Z. Q. Zhou, C. Breen, J. Steckel, V. Bulovic, M. Bawendi, S. Coe-Sullivan, P. T. Kazlas, High-efficiency quantum-dot light-emitting devices with enhanced charge injection. *Nat. Photonics* **7**, 407–412 (2013).
41. D. H. Lee, Y. P. Liu, K. H. Lee, H. Chae, S. M. Cho, Effect of hole transporting materials in phosphorescent white polymer light-emitting diodes. *Org. Electron.* **11**, 427–433 (2010).
42. J. H. Jo, J. H. Kim, K. H. Lee, C. Y. Han, E. P. Jang, Y. R. Do, H. Yang, High-efficiency red electroluminescent device based on multishelled InP quantum dots. *Opt. Lett.* **41**, 3984–3987 (2016).
43. H. W. Hu, G. Haider, Y. M. Liao, P. K. Roy, R. Ravindranath, H. T. Chang, C. H. Lu, C. Y. Tseng, T. Y. Lin, W. H. Shih, Y. F. Chen, Wrinkled 2D materials: A versatile platform for low-threshold stretchable random. *Adv. Mater.* **29**, 1703549 (2017).
44. T.-M. Sun, C.-S. Wang, C.-S. Liao, S.-Y. Lin, P. Perumal, C.-W. Chiang, Y.-F. Chen, Stretchable random lasers with tunable coherent loops. *ACS Nano* **9**, 12436–12441 (2015).
45. J. Xia, J. He, K. Xie, X. Zhang, L. Hu, Y. Li, X. Chen, J. Ma, J. Wen, J. Chen, Q. Pan, J. Zhang, I. D. Vatnik, D. Churkin, Z. Hu, Replica symmetry breaking in FRET-assisted random laser based on electrospun polymer fiber. *Ann. Phys.* **531**, 1900066 (2019).

46. J. F. Galisteo-López, M. Ibisate, C. López, FRET-tuned resonant random lasing. *J. Phys. Chem. C* **118**, 9665–9669 (2014).
47. K. Shadak Alee, S. Barik, S. Mujumdar, Förster energy transfer induced random lasing at unconventional excitation wavelengths. *Appl. Phys. Lett.* **103**, 221112 (2013).
48. X. Shi, J. Tong, D. Liu, Z. Wang, Resonance energy transfer process in nanogap-based dual-color random lasing. *Appl. Phys. Lett.* **110**, 171110 (2017).
49. L. Cerdán, E. Enciso, V. Martín, J. Bañuelos, I. López-Arbeloa, A. Costela, I. García-Moreno, FRET-assisted laser emission in colloidal suspensions of dye-doped latex nanoparticles. *Nat. Photonics* **6**, 621–626 (2012).
50. C. S. Wang, H. Y. Lin, T. H. Lin, Y. F. Chen, Enhancement of random lasing assisted by light scattering and resonance energy transfer based on ZnO/SnO nanocomposites. *AIP Adv.* **2**, 012133 (2012).
51. S. Kedia, S. Sinha, Random laser emission at dual wavelengths in a donor-acceptor dye mixture solution. *Results Phys.* **7**, 697–704 (2017).
52. G. W. Shu, W. Z. Lee, I. J. Shu, J. L. Shen, J. C. A. Lin, W. H. Chang, R. C. Ruaan, W. C. Chou, Photoluminescence of colloidal CdSe/ZnS quantum dots under oxygen atmosphere. *IEEE Trans. Nanotechnol.* **4**, 632–636 (2005).
53. C. T. Yuan, Y. C. Lin, Y. N. Chen, Q. L. Chiu, W. C. Chou, D. S. Chuu, W. H. Chang, H. S. Lin, R. C. Ruaan, C. M. Lin, Studies on the electronic and vibrational states of colloidal CdSe/ZnS quantum dots under high pressures. *Nanotechnology* **18**, 185402 (2007).
54. W. Yin, N. Kim, J. Jeong, K. S. Kim, H. Chae, T. K. Ahn, Efficient heterotransfer between visible quantum dots. *J. Phys. Chem. C* **121**, 4799–4805 (2017).

**Acknowledgments**
**Funding:** This work was supported by the Ministry of Science and Technology and Ministry of Education of the Republic of China. **Author contributions:** T.-L.S. performed all experiments and wrote the manuscript. H.-W.H. assisted with the experiment of photoluminescence measurement. W.-J.L. and Y.-M.L. assisted with the analysis of electroluminescence experiment. T.-P.C. performed the TRPL measurement. Y.-K.L. assisted with the data analysis. T.-Y.L. assisted with data analysis and mechanism construction of the results. Y.-F.C. developed the idea of the research work, assisted with the data analysis, and discussed the results. **Competing interests:** The authors declare that they have no competing interests. **Data and materials availability:** All data needed to evaluate the conclusions in the paper are present in the paper and/or the Supplementary Materials. Additional data related to this paper may be requested from the authors.

Submitted 11 November 2019
Accepted 24 August 2020
Published 7 October 2020
10.1126/sciadv.aba1705

**Citation:** T.-L. Shen, H.-W. Hu, W.-J. Lin, Y.-M. Liao, T.-P. Chen, Y.-K. Liao, T.-Y. Lin, Y.-F. Chen, Coherent Förster resonance energy transfer: A new paradigm for electrically driven quantum dot random lasers. *Sci. Adv.* **6**, eaba1705 (2020).

Science Advances

# Coherent Förster resonance energy transfer: A new paradigm for electrically driven quantum dot random lasers

Tien-Lin Shen, Han-Wen Hu, Wei-Ju Lin, Yu-Ming Liao, Tzu-Pei Chen, Yu-Kuang Liao, Tai-Yuan Lin and Yang-Fang Chen

*Sci Adv* **6** (41), eaba1705.
DOI: 10.1126/sciadv.aba1705



*Science Advances* (ISSN 2375-2548) is published by the American Association for the Advancement of Science, 1200 New York Avenue NW, Washington, DC 20005. The title *Science Advances* is a registered trademark of AAAS.